

# We are IntechOpen, the world's leading publisher of Open Access books Built by scientists, for scientists

7,200

Open access books available

190,000

International authors and editors

205M

Downloads

Our authors are among the

154

Countries delivered to

TOP 1%

most cited scientists

12.2%

Contributors from top 500 universities



WEB OF SCIENCE™

Selection of our books indexed in the Book Citation Index  
in Web of Science™ Core Collection (BKCI)

Interested in publishing with us?  
Contact [book.department@intechopen.com](mailto:book.department@intechopen.com)

Numbers displayed above are based on latest data collected.  
For more information visit [www.intechopen.com](http://www.intechopen.com)



# Strategies for High Resolution Patterning of Conducting Polymers

Lin Jiang and Lifeng Chi

*Physikalisches Institut Westfälische Wilhelms-Universität Münster & Center for Nanotechnology (CeNTech), 48149 Münster Germany*

## 1. Introduction

The discovery of conducting polymers by MacDiarmid, Shirakawa and Heeger in 1977 has generated enormous interest in  $\pi$ -conjugated macromolecules.<sup>[1]</sup> Since then, their unique properties such as the metal-insulator transition induced by doping-undoping process, controllable optoelectronic property through molecular design and attractive mechanical properties and processing advantages have stimulated many progresses in researches and technically relevant applications. They have been extensively studied allowing the demonstration of different functional devices including organic light emitting diodes (OLED),<sup>[2]</sup> electrochromic devices,<sup>[3]</sup> field effect transistors<sup>[4]</sup> and integrated circuits,<sup>[5]</sup> batteries,<sup>[6]</sup> photodetectors<sup>[7]</sup> and sensors.<sup>[8]</sup> In microelectronic-related device fabrication, conducting polymers need to be patterned into micro- and nanostructures. For example, conducting polymer microstructures are used as interconnects and as source, drain and gate electrodes in all-polymer integrated circuits<sup>[5]</sup> or as red, green, blue (RGB) pixels in multi-color OLED displays.<sup>[9]</sup> In contrast to the striking achievements in conducting polymer microelectronic devices, the application of conducting polymer nanostructures in nanoelectronic devices is still under development due to the current limitation of nanofabrication. However, their applications in other less demanding areas such as optics, sensors and biotechnology have been demonstrated. For example, Boroumand et al. demonstrated a series of electrically driven nanoscale light sources, which might be used in near-field optical communication system and storage devices.<sup>[10]</sup> Roman et al. gave strong evidence that nanopatterning of conducting polymer was capable of improving the performance of photodiodes.<sup>[11]</sup> Matterson demonstrated the increasing efficiency and controllable light output from structured LEDs.<sup>[12]</sup> Recently, several groups reported the use of conducting polymer nanostructures as chemical or biological sensors, which show higher sensitivity than conventional sensors.<sup>[13]</sup> For instance, Craighead and co-workers have reported a polyaniline nanowire chemical sensor more sensitive than the traditional film-based sensors for the detection of ammonium gas.<sup>[14]</sup> Huang et al. reported a nanofiber film sensor that responds much faster than the conventional film sensor to HCl gas.<sup>[15]</sup> Apart from the detection of chemical vapors, improved sensing behaviour is also observed when detecting biological molecules, such as glucose<sup>[16]</sup> and biotin.<sup>[17]</sup>

Source: Lithography, Book edited by: Michael Wang,  
ISBN 978-953-307-064-3, pp. 656, February 2010, INTECH, Croatia, downloaded from SCIYO.COM

There are basically two approaches to fabricating nanoscale conducting polymeric structures: the synthesis and post-assembly method<sup>[18]</sup> or the microfabrication method<sup>[19-22]</sup> (photolithography, soft lithography, etc.). In the former approach, sub-100 nm structures can be readily obtained by either template synthesis<sup>[23]</sup> or electrospinning.<sup>[24]</sup> However, manipulation and positioning of the synthesized nanoscale objects with respect to microelectrodes is rather difficult and not precise. In the latter case, conducting polymers can be precisely patterned by a variety of microlithographic methods based on different principles. For example, soft lithography<sup>[19]</sup> can be used to fabricate conducting-polymer patterns by means of selective deposition, embossing, and so on; photo- or electron (e)-beam-initiated polymerization or degradation<sup>[20]</sup> can define patterns on conducting polymer films; dip-pen lithography<sup>[21]</sup> is capable of patterning conducting polymers, based on a principle of ink transfer from the tip to the substrate; electrochemical lithography<sup>[22]</sup> represents another series of methods of obtaining patterned conducting polymers, which can be obtained by scanning electrochemical microscopy (SECM), electrochemical dip-pen lithography, or scanning tunneling microscopy (STM). Although these microlithographic methods yield conducting-polymer micro/nanostructures, the methods which are capable of integrating high resolution with high throughput are still highly demanded.

In this review article, we intent to summarize our recent works in high resolution patterning of conducting polymers. Three different strategies will be included, together with the demonstration of advanced functions, e.g. in gas sensing and anisotropic conducting performance.

## **2. Surfactant assisted fabrication of polypyrrole nanowires between microelectrodes**

Since conductive/semiconductive polymers are promising candidates for future molecular electronics, opto-electronics, and electro-optics, the reproducible fabrication of these materials on pre-defined positions, e.g. between microelectrodes, attracts increased scientific and technological attentions. To achieve this goal, one of the key issues has to be addressed: the improvement of the adhesion of the conducting polymers to the substrate without reducing the conductivity, especially with insulating surfaces. We used firstly a strategy by employing both surfactants and surface coupling reagents. E-beam as well as AFM lithography was used to create defined surface patterns. The successful construction of PPy structures (20-120 nm in thickness and down to 200 nm in width) was achieved.

It has been demonstrated that polypyrrole synthesized in the presence of surfactants is superior to that polymerized in the presence of small inorganic anions because anionic surfactants induce structural regularity into the polymers<sup>[23]</sup> These amphiphilic molecules inside the polypyrrole films will also help to improve the adhesion of polypyrrole to the substrate.<sup>[23a]</sup> Another way to immobilize polypyrrole is to treat the substrate with a surface-reactive reagent bearing pyrrole, for example, N-(3-trimethoxysilylpropyl) pyrrole (abbreviated as py-silane). Polymerization in the presence of a self-assembled monolayer of this reagent yields a polypyrrole film that is more adherent to the substrate.<sup>[24]</sup> We found that only the employment of both surfactant and py-silane would result in satisfying submicrometer structures, with the surfactant helping to wet the substrate and py-silane helping to immobilize the polypyrrole film.

First, we utilized an e-beam or tip-scratching to define channels in the resist of poly(methyl methacrylate) (PMMA) on a silicon substrate. Second, we modified the patterned wafer with

py-silane by placing the wafer into py-silane vapor at 140 mbar for 20 min. Third, we covered this wafer with a layer of oxidant solution, which was prepared by dissolving iron chloride (0.5 g) and sodium dodecyl sulfate (SDS; 0.125 g) in purified water (2.5 mL) by either spin-coating or immersion. Then, the wafer was exposed to pyrrole vapor to induce the polymerization. Finally, the resist and the polypyrrole on top of it were removed while the polypyrrole directly in contact with the silicon substrate remained.

Since this method offers the opportunity to grow polypyrrole wires in situ at a desired position, submicrometer wires can thus be introduced between two microelectrodes. We first fabricated gold electrodes by standard e-beam lithographic patterning. The PMMA was spin-coated onto this wafer. Using AFM-tip scratching, the coated PMMA between the electrodes was selectively removed to form a channel. The polypyrrole wire and microelectrode contacts can be generated with different dimensions within this channel by post-polypyrrole growth and using a lift-off process. For example, a polypyrrole wire (500 nm wide, 2.5 mm long, and 60 nm thick) that bridges two electrodes is shown in Figure 1a. In order to confirm the contact between the polypyrrole wire and the electrodes, current and voltage studies were carried out. As a control, we also studied the junction before polypyrrole growth, as shown in Figure 1b (dashed line), which indicates that it has no conductance. After polypyrrole growth, a linear dependence of the current on the applied potential was observed (Figure 1b, solid line), thus confirming the ohmic contact. The conductivity of this wire was calculated to be 0.8–1.2  $\text{Scm}^{-1}$ , which is comparable with that of the bulk polymer. Polypyrrole wires as small as 250 nm in width and 120 nm in thickness, which grew in the channel defined by e-beam lithography, can also be fabricated.

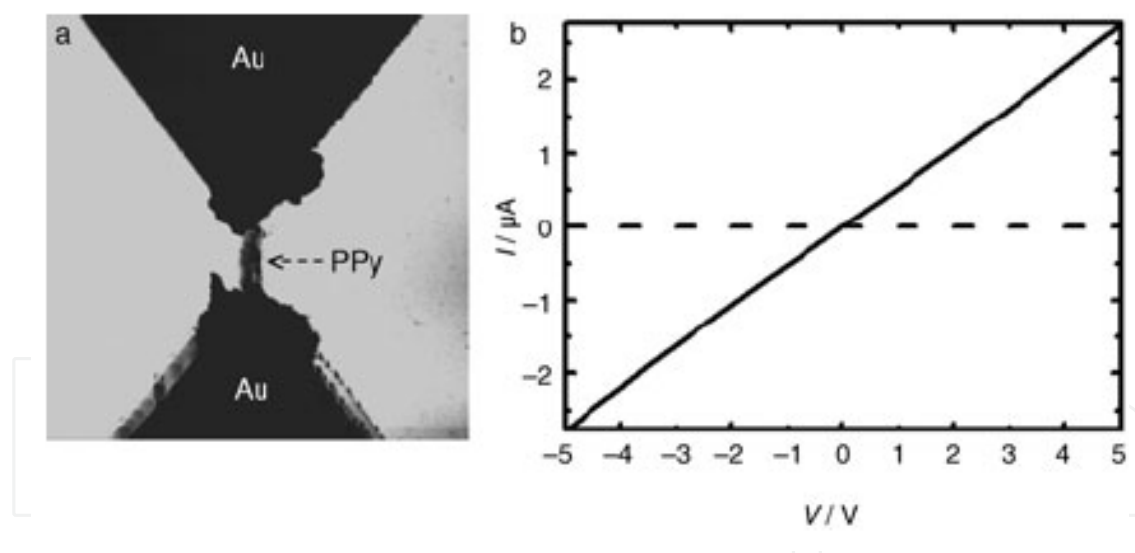


Fig. 1. a) AFM image of a 500-nm-wide polypyrrole wire grown between Au electrodes (image=10-10  $\text{mm}^2$ ); b) I-V characteristics of this junction before (b) and after (c) polypyrrole wire growth.

In order to clarify the functions of both SDS and py-silane during the construction process, we performed two control experiments. First, fabrication was carried out in the absence of py-silane. It was found that SDS-doped polypyrrole had only limited adhesion to the substrate, as evidenced by the fact that only structures on the micrometer scale, rather than with features of several hundred nanometers could be fabricated. We attributed this result to the weak adhesion based on the physical adsorption between SDS-doped polypyrrole and

the substrate when the contact area was in the submicrometer scale. Second, we employed only py-silane. There is no doubt that py-silane will immobilize the polypyrrole onto the substrate through covalent bonds. However, submicrometer wire formation was not observed because the oxidant solution without SDS will not wet the substrate. Hence, based on the above observations, successful fabrication requires the combination of both SDS and the pyrrole-bearing silane.

### 3. High resolution and high throughput patterning based on a random copolymer strategy

Due to a lack of control over the film thickness during deposition the introduced above is not suitable for high-resolution (< 100 nm) fabrication. We further developed a copolymer strategy to control the thickness and the adhesive and electrical properties of conducting polymers by incorporating a surface-active monomer into the main chains. The method is suitable for the fabrication of devices with a sub-100 nm resolution, and allows the device exclusively based on conducting polymers. Combining with nanoimprinting lithography (NIP), high resolution of conductive polymers with high throughput become then possible. Figure 2 depicts the fabrication process, which, in accordance with the standard lift-off process, includes three steps. In the first step, a pattern is defined on the photoresist using e-beam lithography or NIP. Second, a copolymer film thinner than the resist layer is deposited by oxidizing pyrrole (or aniline) and Py-silane with iron chloride. Finally, the resist is lifted off in acetone by sonication.

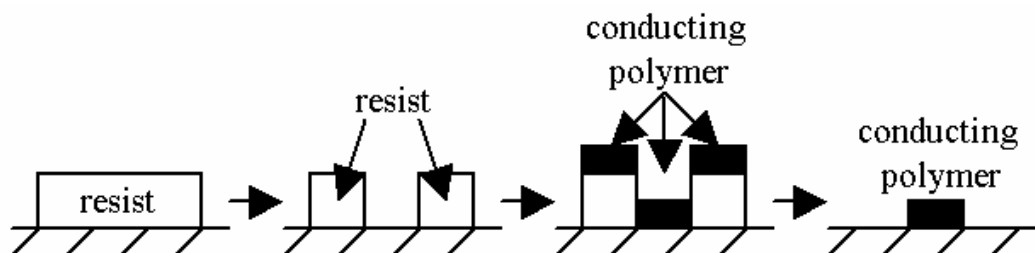


Fig. 2. Schematic representation of the fabrication process.

In order to realize successful fabrication of conducting-polymer structures by the lift-off process and to facilitate their further application as sensors, conductivity and adhesion, as well as their combination, are the essential parameters that should be taken into account. Here we employed the two-point measurement method and the adhesion-tape test<sup>[19c]</sup> to estimate the electrical and adhesive properties of the copolymer film, respectively. Taking polypyrrole as an example, the introduction of py-silane has a significant influence on the properties of polypyrrole. Notably, copolymers that contain py-silane (9 vol.-%) can successfully withstand the adhesion-tape test whereas pure polypyrrole cannot. Moreover, upon increasing the fraction of py-silane, electrical conductivity and film thickness of the copolymer decrease.<sup>[25]</sup> The film thickness can be controlled by the deposition time,<sup>[19c]</sup> thus it can be kept thinner than the resist layer, thereby facilitating the lift-off process. In order to obtain a strongly adherent film that retained as high conductivity as possible, we carried out all depositions at a pyrrole to py-silane volume ratio of 91:9 unless stated otherwise. Under these conditions, the actual copolymer composition is estimated to be roughly 97:3 (pyrrole to py-silane),<sup>[25]</sup> based on X-ray photoelectron spectroscopy (XPS) measurements.

Construction of sub-100 nm conducting polymer structures on insulating surfaces is normally hardly achievable by microlithographic techniques, except for a few examples.<sup>[20c]</sup> The strategy presented here offers efficient fabrication of conducting-polymer structures with a resolution of less than 100 nm. For example, we were able to fabricate an 80 nm wide, 11  $\mu\text{m}$  long polypyrrole nanowire on a silicon substrate with a 100 nm thermally oxidized SiO<sub>2</sub> layer (Figure 3a). The wire structure was initially defined on the resist by e-beam lithography.

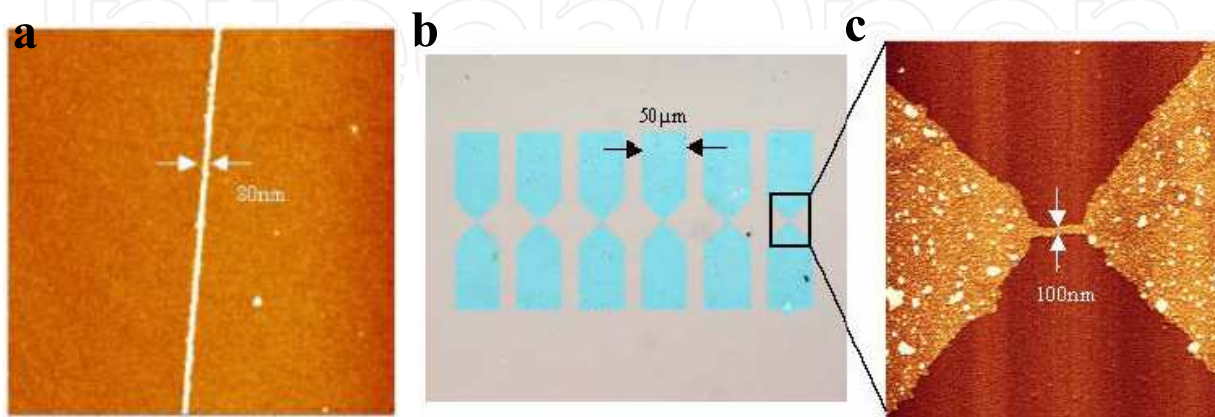


Fig. 3. a) Atomic force microscopy (AFM) image of an 80 nm wide polypyrrole wire (image size: 11  $\mu\text{m}$   $\times$  11  $\mu\text{m}$ ). b) Optical images of six pairs of polypyrrole microelectrode shaped structures (size: 475  $\mu\text{m}$   $\times$  390  $\mu\text{m}$ ). c) Enlarged AFM image of the area inside the black box of Figure 2b, showing one 100 nm wide polypyrrole wire that bridges the ends of two polypyrrole microelectrodes (size: 9  $\mu\text{m}$   $\times$  10  $\mu\text{m}$ ).

Precise manipulation and placement of the nanostructures at desired locations and their integration with larger-scale systems has long been a challenge and proposes a serious hindrance for the further development of nanoelectronics.<sup>[18]</sup> Exploiting advantages of the copolymer strategy, our nanowires can be integrated in between the conducting-polymer microelectrodes in one deposition step, facilitating the fabrication of nanosensors exclusively based on polymers. Figure 3b shows an optical image of six pairs of polypyrrole microelectrodes on a silicon substrate with a 100 nm SiO<sub>2</sub> layer (structures defined by e-beam lithography). The polypyrrole nanowires in between the microelectrodes are not visible at this magnification. The overall electrodes consist of homogeneous, closely packed, globular-shaped polypyrrole structures (see for example Figure. 3c, electrode part). All six pairs of electrodes were successfully connected with polypyrrole nanowires, proving the reliability of this strategy. In Figure 3c one of the six junctions, consisting of one single polypyrrole nanowire (100 nm wide, 1.25  $\mu\text{m}$  long) bridging the ends of two polypyrrole microelectrodes, is shown.

By combining the copolymer strategy presented above with NIP, we successfully fabricated high density, large area conducting polymer nanostructures with a resolution of 100 nm (see Figure 4a). Each field of polypyrrole nanowires can extend over a large area, as seen in the light diffraction images captured by a CCD camera shown in Figure 4b. Position 1, 2, 3, 4, 5 and 6 correspond to 100, 150, 250, 350, 320 and 220 nm wide polypyrrole nanowires separated by 150, 200, 300, 400, 380 and 280 nm, respectively. The uniformity of each color reflects a good uniformity of each nanowire array.

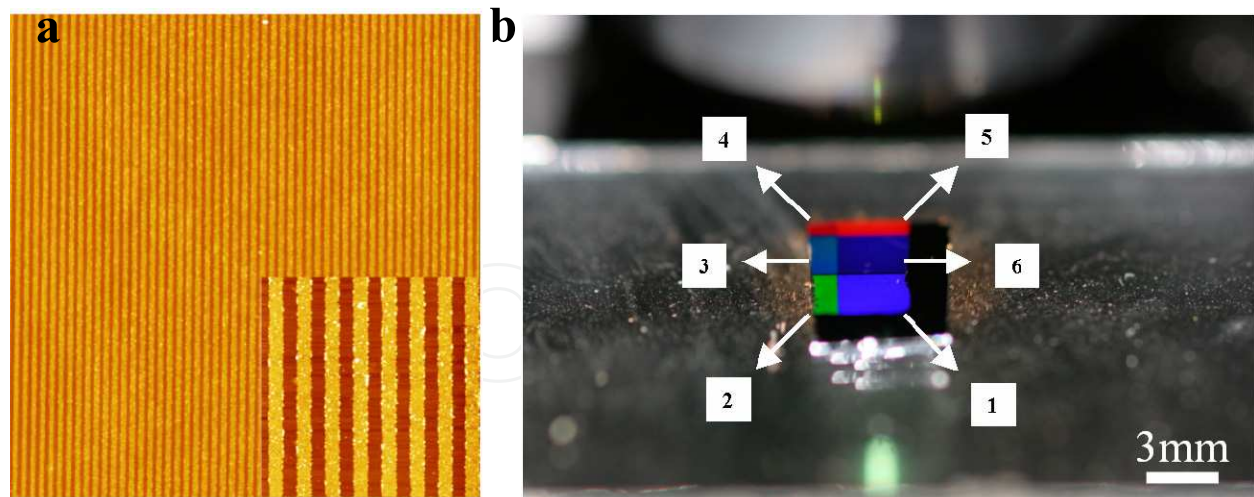


Fig. 4. a) 150 nm wide polypyrrole nanowires with a separation of 150 nm (size:  $30 \times 30 \mu\text{m}^2$ ). Inset: enlarged AFM image showing one  $5 \times 5 \mu\text{m}^2$  area; b) CCD image showing the light diffraction from high density polypyrrole nanowires fabricated by NIL and a lift off process. (1) 100 nm wide polypyrrole nanowires separated by 150 nm. (2) 150 nm wide polypyrrole nanowires separated by 200 nm. (3) 250 nm wide polypyrrole nanowires separated by 300 nm. (4) 350 nm wide polypyrrole nanowires separated by 400 nm. (5) 320 nm wide polypyrrole nanowires separated by 380 nm. (6) 220 nm wide polypyrrole nanowires separated by 280 nm.

To demonstrate the functionality of this structure, a current-versus-potential ( $I$ - $V$ ) study was carried out. A linear dependence of the current on the applied potential was observed (Figure 5a), confirming the ohmic behavior of the material. We further evaluated the sensing performance of this device by exposing it to a 240 ppm  $\text{NH}_3$  stream. The detection of  $\text{NH}_3$  in air is of interest from an environmental point of view because of the high toxicity of this gas. The sensing principle is based on the fact that the electron-donating molecule (in this case  $\text{NH}_3$ ) can reduce the charge-carrier concentration of polypyrrole (a p-type conducting polymer or electron acceptor) and decrease its conductivity.<sup>[26]</sup> The device shown in Figure 5c exhibits a reversible response upon the addition of  $\text{NH}_3$  with a sensitivity (defined as  $R/R_0 - 1$ , where  $R_0$  is the initial resistance and  $R$  is the resistance after exposure to  $\text{NH}_3$ ) of

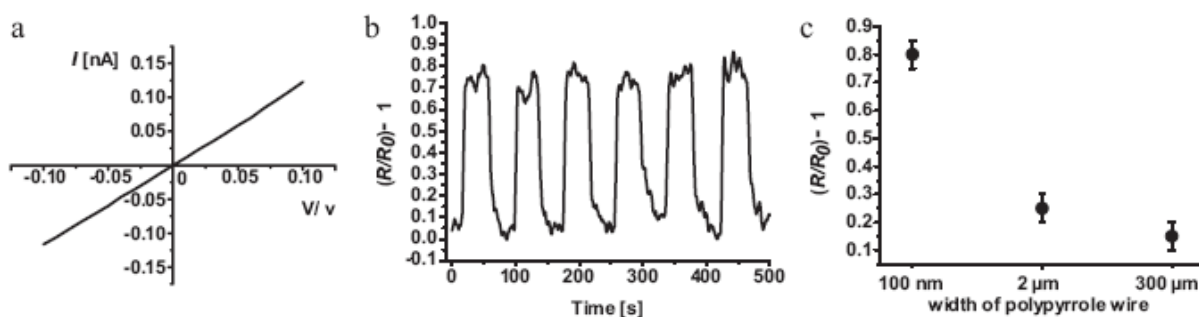


Fig. 5. a)  $I$ - $V$  characteristics of a 100 nm nanodevice consisting exclusively of polypyrrole as shown in Figure 3c. b) Real-time response ( $R/R_0 - 1 =$  sensitivity, see text) of this 100 nm nanowire sensor (Fig. 3c) to a 240 ppm  $\text{NH}_3$  stream (40 s on/40 s off). c) Sensitivity dependence on the width of the wire between the electrodes (at constant thickness).

0.8 (Figure 5b), which is of the same order of magnitude as reported for polypyrrole-based sensors.<sup>[27]</sup> This value can be further improved by the introduction of other anionic dopants.<sup>[27]</sup> We have compared the sensitivity of this nanosensor consisting exclusively of polypyrrole with a polypyrrole-nanowire sensor with metal electrode contacts and observed no difference, indicating that the nanowire is the key element that determines the sensitivity. By increasing the width of the wire from the nanometer regime to the micrometer (e.g., 2  $\mu\text{m}$  in width) or even into bulk, a decrease in sensitivity was observed (Figure 5c), proving the superiority of the nanoscale device. This is most likely due to the high surface area to volume ratio of the nanowire. A conductivity enhancement trend was also observed with decreased wire width (data not shown here), which is in agreement with results reported in literature.

With the large area conductive polymer structures based on the NIP patterns, the electronic connection became quite straightforward: They may be easily addressed electrically by connection to suitably sized metal electrodes. Moreover, since the residual layer is not

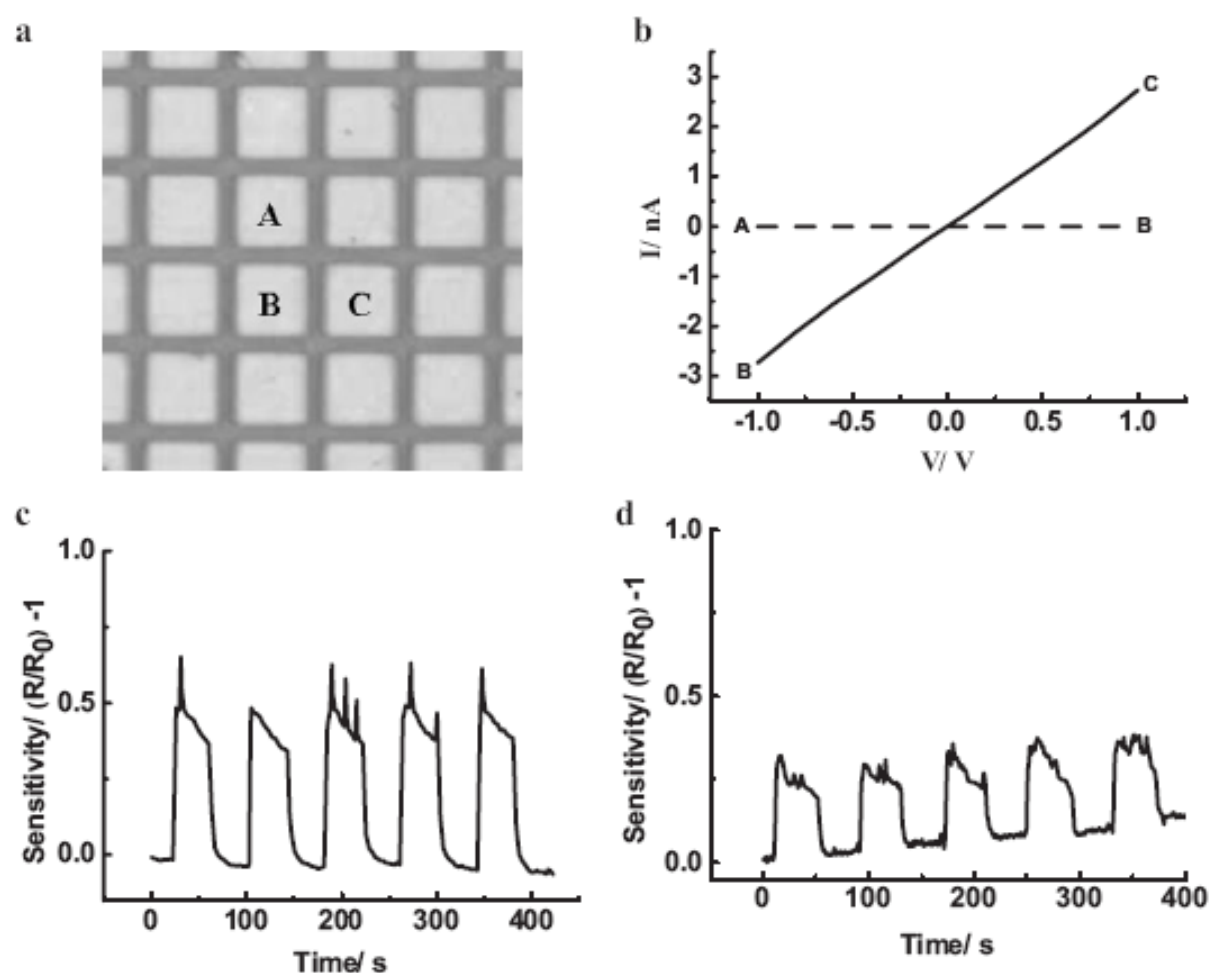


Fig. 6. a) Optical image of the gold pads evaporated on the nanowire arrays (image size: 330  $\mu\text{m} \times 330 \mu\text{m}$ ). b) Resistance parallel (BC solid line) and perpendicular (AB dashed line) to the nanowire direction (BC direction). The measured anisotropy ratio is  $1.6 \times 10^3$ . c) Real-time response of a sensor consisting of 300 nm nanowire arrays to a 240 ppm  $\text{NH}_3$  stream (40 s on/40 s off). d) Real-time response of a sensor consisting of 5  $\mu\text{m}$  wire arrays to a 240 ppm  $\text{NH}_3$  stream (40 s on/40 s off).



present, this should guarantee high resistance anisotropy in the parallel and perpendicular directions. Taking into account the sensing properties of conducting polymers, these electrically addressable conducting polymer nanowires could be directly used as nanosensors. For nanosensor applications, the high density nanowires offer a high error tolerance in the device performance if one or several nanowire fabrication failures occur.

In order to demonstrate the above advantages, gold pads were deposited on the nanowire arrays by shadow mask evaporation (Figure 6a). Figure 6b shows the typical current-voltage curves measured from the 300 nm wide nanowire arrays. As expected, the resistance in the parallel and perpendicular directions shows great anisotropy. Resistance values of 370 M $\Omega$  and 600 G $\Omega$  were obtained parallel and perpendicular to the nanowire direction, respectively, resulting in a value of  $1.6 \times 10^3$  for the anisotropy ratio. The resistance varied from 200 to 400 M $\Omega$  for different wire arrays. These isolated electrically addressable wire arrays could be directly used as nanowire sensors. A demonstration of their sensing potential is shown in Figure 6c and d. Note that the electrical addressing of the nanowire array can also be realized by connecting them with silver glue and so on, because the nanowire array can extend over a larger area. Given the advantages of NIL, we thus developed a facile method to fabricate conducting-polymer nanosensors at low cost.

#### 4. Scaling down from micrometer patterns to nanometer structures

In the combination of NIL and copolymer strategy introduced above, the conducting polymer (CP) layer must be thinner than the resist layer for a successful lift-off.<sup>[28]</sup> It restricts the construction of CPs with arbitrary thickness, which sometimes limits the application of the resulting polymer patterns. Furthermore, in NIL, the imprinted structure is usually a negative copy of the stamp. Thus, a high resolution stamp is required for creating a high resolution pattern, which leads to an expensive and time-consuming fabrication process. Herein, we demonstrate an approach to reduce the lateral size of CP structures using an isotropic plasma etching (IPE). Using this method, we are able to improve the printed pattern resolution without the thickness limit of the CP layer, and the CP can be protected from the etching process.

The fabrication process is illustrated in Figure 7. First, the polyaniline (PANI) layer was deposited onto a silicon dioxide (or quartz) substrate. Then a 400-nm poly(methyl methacrylate) (PMMA) film was spin-coated on the PANI film. Subsequently, the stamp was pressed into the PMMA film heated above  $T_g$ , followed by peeling away from the substrate after cooling down the system. Figure 8a is an atomic force microscopy (AFM) image of the line patterns on the stamp with gradually changing channel width, which ranges from 1.4  $\mu\text{m}$  to 2.6  $\mu\text{m}$ . The stamp pattern can be completely transferred into the PMMA film by the above printing processes as presented in Figure 8b. Anisotropic plasma etching (APE) is usually used for faithful pattern transferring rather than IPE because IPE will also etch off the profiles of protrusions at the same time as the residual layer. In our case, we expect to scale down the lateral dimension of the CP pattern when removing the residual PMMA and the PANI covered by the residual PMMA using IPE. The width correlation of the produced PANI line and the imprinted PMMA line is illustrated in Figure 9. It is evidently demonstrated that by using a stamp features larger than 1  $\mu\text{m}$ , one can scale down till 250 nm. No obviously changes in UV-Vis spectrum indicated that PANI remained intact after by the imprinting and etching process.

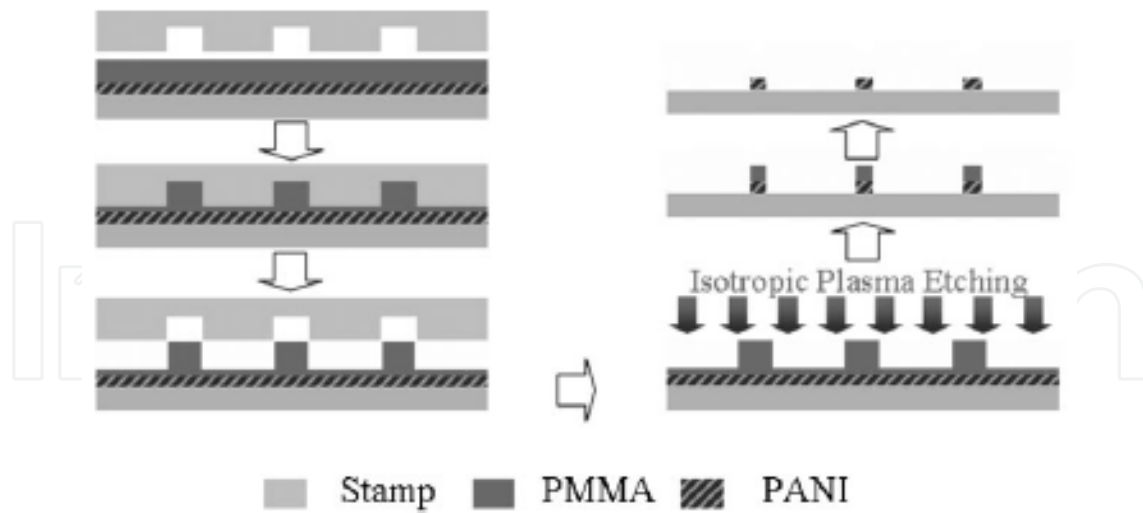


Fig. 7. Schematic illustration of the fabricating process with NIL.

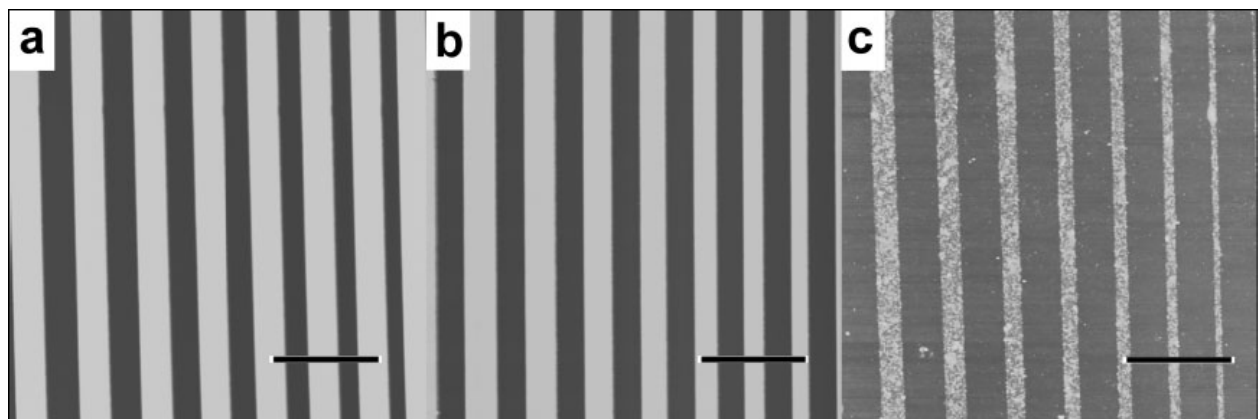


Fig. 8. AFM images of (a) the silicon stamp, (b) an imprinted PMMA structure using the stamp shown in (a), and (c) fabricated PANI structures with NIL (Scale bar  $\frac{1}{4}$ 7.5mm).

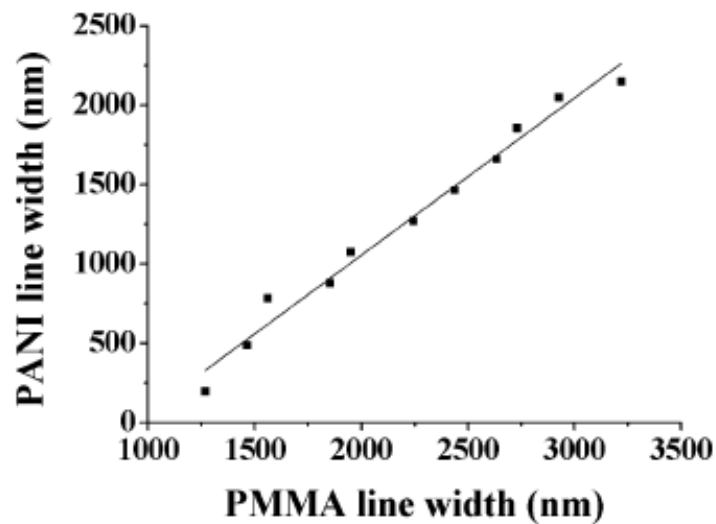


Fig. 9. The width correlation of the produced PANI line and the imprinted PMMA line.

The charged PANI structure is an ideal candidate for selective absorption of the negatively charged particles. As shown in Figure 10, Silver nanoparticles (SNPs) were selectively adsorbed on the patterned PANI. Previous investigation shows that electrostatic interaction is the main interaction between the sodium citrate-covered SNPs and the substrate, [29,30] and that the suitable pH of the particle solution is between 2 and 4. [31-33] The SNP patterns were obtained by keeping the PANI patterned substrate in the SNP aqueous solution (pH 3) for several hours. The result demonstrates that the PANI pattern is of high selectivity for SNP adsorption.

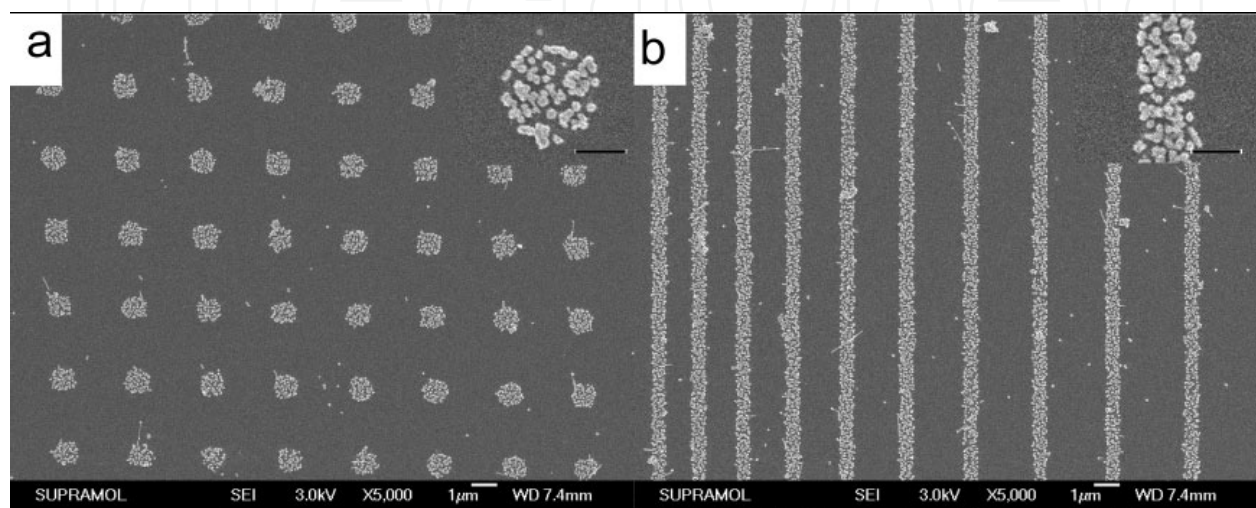


Fig. 10. SEM images of SNPs adsorbed onto the PANI dots (a) and lines (b). Scale bar=1 μm. Scale bar of the insets=500 nm.

## 5. Summary and outlook

We introduce here three different strategies to fabricate ordered conductive polymer structures with high special resolution and high throughput. The advanced functions in e.g. sensitive gas sensing are demonstrated. The methods presented above should be general to pattern other functional polymers. However, even we are able to achieve the resolution till 80 nm, the reproducibility below 100 nm remains a problem. Improvement of the presented methods are on going. For instance, for copolymer strategy, by using warm bathing the silane can be hydrolyzed adequately. Only few amount of py-silane (0.08 vol.-%) is needed for adhesion of copolymer film thus results in a significantly increase of the electrical conductivity and a decrease of the polymer film thickness. By such an improvement, the smallest feature size of ppy wire can be reduced to 50nm with well reproducibility. The investigation on conductivity of polymer wires well below 100 nm will be a very interesting topic both for theoretical study and practice use.

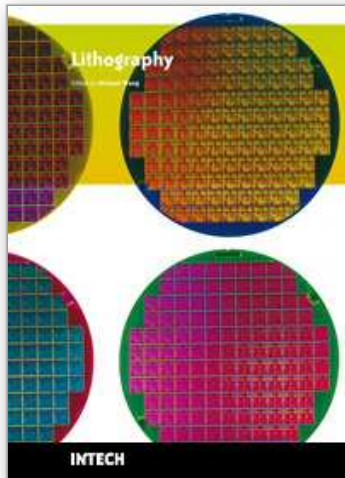
## 6. References:

- [1] for reviews, see: a) H. Shirakawa, *Angew. Chem. Int. Ed.* 2001, 40, 2574. b) A. G. MacDiarmid, *Angew. Chem. Int. Ed.* 2001, 40, 2581. c) A. J. Heeger, *Angew. Chem. Int. Ed.* 2001, 40, 2591.

- [2] J. H. Burroughes, D. D. C. Bradley, A. R. Brown, R. N. Marks, K. Mackay, R. H. Friend, P. L. Burns, A. B. Holmes, *Nature* 1990, 347, 539-541.
- [3] a) G. Sonmez, C. K. F. Shen, Y. Rubin, F. Wudl, *Angew. Chem. Int. Ed.* 2004, 43, 1498. b) G. Sonmez, H. B. Sonmez, C. K. F. Shen, F. Wudl, *Adv. Mater.* 2004, 16, 1905.
- [4] a) F. Garnier, R. Hajlaoui, A. Yassar, P. Srivastava, *Science*, 1994, 265, 1684-1686. b) Z. Bao, Y. Feng, A. Dodabalapur, V. R. Raju, A. J. Lovinger, *Chem. Mater.* 1997, 9, 1299-1301.
- [5] C. J. Drury, C. M. J. Mutsaers, C. M. Hart, M. Matters, D. M. de Leeuw, *Appl. Phys. Lett.* 1998, 73, 108-110.
- [6] C. Arbizzani, M. Mastragostino, S. Panero, P. Prospero, B. Scrosati, *Synth. Met.* 1989, 28, C663.
- [7] C. H. Lee, G. Yu, C. Zhang, A. J. Heeger, *Appl. Phys. Lett.* 1994, 64, 1540.
- [8] C. G. J. Koopal, B. Ruiters, R. J. M. Nolte, *J. Chem. Soc. Chem. Commun.* 1991, 1691.
- [9] C. D. Mueller, A. Falcou, N. Reckefuss, M. Rojahn, V. Wiederhirm, P. Rudati, H. Frohne, O. Nuyken, H. Becker, K. Meerholz, *Nature* 2003, 421, 829.
- [10] F. A. Boroumand, P. W. Fry, D. G. Lidzey, *Nano Lett.* 2005, 5, 67.
- [11] L. S. Roman, O. Inganäs, T. Granlund, T. Nyberg, M. Svensson, M. R. Andersson, J. C. Hummelen, *Adv. Mater.* 2000, 12, 189.
- [12] B. J. Matterson, J. M. Lupton, A. F. Safonov, M. G. Salt, W. L. Barnes, I. D. W. Samuel, *Adv. Mater.* 2001, 13, 123.
- [13] a) M. H. Yun, N. V. Myung, R. P. Vasquez, C. Lee, E. Menke, R. M. Penner, *Nano Lett.* 2004, 4, 419. b) K. Ramanathan, M. A. Bangar, M. H. Yun, W. Chen, A. Mulchandani, N. V. Myung, *Nano Lett.* 2004, 4, 1237. c) K. Ramanathan, M. A. Bangar, M. H. Yun, W. Chen, N. V. Myung, A. Mulchandani, *J. Am. Chem. Soc.* 2005, 127, 496. d) X. Y. Wang, Y. G. Kim, C. Drew, B. C. Ku, H. Kumar, L. A. Samuelson, *Nano Lett.* 2004, 4, 331. e) H. Q. Liu, J. Kameoka, D. A. Czaplewski, H. G. Craighead, *Nano Lett.* 2004, 4, 671. f) J. X. Huang, S. Virji, B. H. Weiller, R. B. Kaner, *J. Am. Chem. Soc.* 2003, 125, 314. g) Y. F. Ma, J. M. Zhang, G. J. Zhang, H. X. He, *J. Am. Chem. Soc.* 2004, 126, 7097. h) E. S. Forzani, H. Q. Zhang, L. A. Nagahara, I. Amlani, R. Tsui, N. J. Tao, *Nano Lett.* 2004, 4, 1785-1788.
- [14] H. Q. Liu, J. Kameoka, D. A. Czaplewski, H. G. Craighead, *Nano Lett.* 2004, 4, 671.
- [15] J. X. Huang, S. Virji, B. H. Weiller, R. B. Kaner, *J. Am. Chem. Soc.* 2003, 125, 314.
- [16] E. S. Forzani, H. Q. Zhang, L. A. Nagahara, I. Amlani, R. Tsui, N. J. Tao, *Nano Lett.* 2004, 4, 1785.
- [17] K. Ramanathan, M. A. Bangar, M. H. Yun, W. Chen, N. V. Myung, A. Mulchandani, *J. Am. Chem. Soc.* 2005, 127, 496.
- [18] See, for example: a) Y. Huang, X. F. Duan, Q. Q. Wei, C. M. Lieber, *Science* 2001, 291, 630. b) P. A. Smith, C. D. Nordquist, T. N. Jackson, T. S. Mayer, B. R. Martin, J. Mbindyo, T. E. Mallouk, *Appl. Phys. Lett.* 2000, 77, 1399.
- [19] a) Y. N. Xia, G. M. Whitesides, *Angew. Chem. Int. Ed.* 1998, 37, 550. b) C. B. Gorman, H. A. Biebuyck, G. M. Whitesides, *Chem. Mater.* 1995, 7, 526. c) Z. Y. Huang, P. C. Wang, A. G. MacDiarmid, Y. N. Xia, G. M. Whitesides, *Langmuir* 1997, 13, 6480. d) K. M. Vaeth, R. J. Jackman, A. J. Black, G. M. Whitesides, K. F. Jensen, *Langmuir* 2000, 16, 8495.
- [20] a) J. Y. Bai, C. M. Snively, W. N. Delgass, J. Lauterbach, *Adv. Mater.* 2002, 14, 1546. b) F. Shi, B. Dong, D. L. Qiu, J. Q. Sun, T. Wu, X. Zhang, *Adv. Mater.* 2002, 14, 805. c) S. H. M. Persson, P. Dyreklev, O. Inganäs, *Adv. Mater.* 1996, 8, 405.

- [21] a) J. H. Lim, C. A. Mirkin, *Adv. Mater.* 2002, 14, 1474. b) M. Su, M. Aslam, L. Fu, N. Q. Wu, V. P. Dravid, *Appl. Phys. Lett.* 2004, 84, 4200.
- [22] a) A. J. Bard, F. R. F. Fan, J. Kwak, O. Lev, *Anal. Chem.* 1989, 61, 132. b) B. W. Maynor, S. F. Filocamo, M. W. Grinstaff, J. Liu, *J. Am. Chem. Soc.* 2002, 124, 522. c) R. Yang, D. F. Evans, W. A. Hendrickson, *Langmuir* 1995, 11, 211.
- [23] a) E. L. Kupila, J. Kankare, *Synth. Met.* 1995, 74, 241–249; b) Y. Kudoh, *Synth. Met.* 1996, 79, 17–22; c) J. P. Pouget, Z. Oblakowski, Y. Nogami, P. A. Albouy, M. Laridjani, E. J. Oh, Y. Min, A. G. MacDiarmid, J. Tsukamoto, T. Ishiguro, A. J. Epstein, *Synth. Met.* 1994, 65, 131–140; d) A. J. Epstein, J. Joo, R. S. Kohlman, G. Du, A. G. MacDiarmid, E. J. Oh, Y. Min, J. Tsukamoto, H. Kaneko, J. P. Pouget, *Synth. Met.* 1994, 65, 149–157; e) J. P. Pouget, C. H. Hsu, A. G. MacDiarmid, A. J. Epstein, *Synth. Met.* 1995, 69, 119–120.
- [24] a) R. A. Simon, A. J. Ricco, M. S. Wrighton, *J. Am. Chem. Soc.* 1982, 104, 2031–2034; b) R. J. Willicut, R. L. McCarley, *J. Am. Chem. Soc.* 1994, 116, 10823–10824; c) C. O. Noble, R. L. McCarley, *J. Am. Chem. Soc.* 2000, 122, 6518–6519.
- [25] a) J. R. Reynolds, P. A. Poropatic, R. L. Toyooka, *Macromolecules* 1987, 20, 958. b) D. Stanke, M. L. Hallensleben, L. Toppare, *Synth. Met.* 1995, 72, 89. c) D. Stanke, M. L. Hallensleben, L. Toppare, *Synth. Met.* 1995, 72, 167. d) D. Stanke, M. L. Hallensleben, L. Toppare, *Synth. Met.* 1995, 73, 261.
- [26] a) J. P. Blanc, N. Derouiche, A. El Hadri, J. P. Germain, C. Maleysson, H. Robert, *Sens. Actuators, B* 1990, 1, 130. b) J. Janata, M. Josowicz, D. M. DeVaney, *Anal. Chem.* 1994, 66, 207R.
- [27] a) H. Nagase, K. Wakabayashi, T. Imanaka, *Sens. Actuators B* 1993, 14, 596. b) M. Brie, R. Turcu, C. Neamtu, S. Pruneanu, *Sens. Actuators, B* 1996, 37, 119.
- [28] S. Y. Chou, P. R. Krauss, P. J. Renstrom, *Appl. Phys. Lett.* 1995, 67, 3114.
- [29] L. Y. Wang, X. H. Ji, X. T. Zhang, Y. B. Bai, T. J. Li, Z. Z. Zhi, X. G. Kong, Y. C. Liu, *Chem. J. Chinese U.* 2002, 23, 2169.
- [30] T. Yonezawa, S. Onoue, T. Kunitake, *Adv. Mater.* 1998, 10, 414.
- [31] D. W. Thompson, I. R. Collins, *J. Colloid Interface Sci.* 1992, 152, 197.
- [32] J. C. Chiang, A. G. MacDiarmid, *Synth. Met.* 1986, 13, 193.
- [33] A. G. Macdiarmid, J. C. Chiang, A. F. Richter, A. J. Epstein, *Synth. Met.* 1987, 18, 285.

IntechOpen



## **Lithography**

Edited by Michael Wang

ISBN 978-953-307-064-3

Hard cover, 656 pages

**Publisher** InTech

**Published online** 01, February, 2010

**Published in print edition** February, 2010

Lithography, the fundamental fabrication process of semiconductor devices, plays a critical role in micro- and nano-fabrications and the revolution in high density integrated circuits. This book is the result of inspirations and contributions from many researchers worldwide. Although the inclusion of the book chapters may not be a complete representation of all lithographic arts, it does represent a good collection of contributions in this field. We hope readers will enjoy reading the book as much as we have enjoyed bringing it together. We would like to thank all contributors and authors of this book.

### **How to reference**

In order to correctly reference this scholarly work, feel free to copy and paste the following:

Lin Jiang and Lifeng Chi (2010). Strategies for High Resolution Patterning of Conducting Polymers, Lithography, Michael Wang (Ed.), ISBN: 978-953-307-064-3, InTech, Available from:  
<http://www.intechopen.com/books/lithography/strategies-for-high-resolution-patterning-of-conducting-polymers>

**INTECH**  
open science | open minds

### **InTech Europe**

University Campus STeP Ri  
Slavka Krautzeka 83/A  
51000 Rijeka, Croatia  
Phone: +385 (51) 770 447  
Fax: +385 (51) 686 166  
[www.intechopen.com](http://www.intechopen.com)

### **InTech China**

Unit 405, Office Block, Hotel Equatorial Shanghai  
No.65, Yan An Road (West), Shanghai, 200040, China  
中国上海市延安西路65号上海国际贵都大饭店办公楼405单元  
Phone: +86-21-62489820  
Fax: +86-21-62489821

© 2010 The Author(s). Licensee IntechOpen. This chapter is distributed under the terms of the [Creative Commons Attribution-NonCommercial-ShareAlike-3.0 License](#), which permits use, distribution and reproduction for non-commercial purposes, provided the original is properly cited and derivative works building on this content are distributed under the same license.

IntechOpen

IntechOpen